JOURNAL OF MATERIALS SCIENCE: MATERIALS IN MEDICINE **15** (2004) 1297–1307

In vitro study on bone formation and surface topography from the standpoint of biomechanics

H. KAWAHARA[1]*, Y. SOEDA[1], K. NIWA[1], M. TAKAHASHI[1], D. KAWAHARA[1], N. ARAKI[2]
[1]*Institute of Clinical Materials, Japan*
E-mail: icm@sea.plala.or.jp
[2]*Department of Histology and Cell Biology, Kagawa Medical University, Japan*

Effect of surface topography upon cell-adhesion, -orientation and -differentiation was investigated by *in vitro* study on cellular responses to titanium substratum with different surface roughness. Cell-shape, -function and -differentiation depending upon the surface topography were clarified by use of bone formative group cells (BFGCs) derived from bone marrow of beagle's femur. BFGCs consisted of hematopoietic stem cells (HSC) and osteogenetic stem cells (OSC). Cell differentiation of BFGCs was expressed and promoted by structural changes of cytoskeleton, and cell-organella, which was caused by mechanical stress with cytoplasmic stretching of cell adhesions to the substratum. Phagocytic monocytes of HSC differentiated to osteomediator cells (OMC) by cytoplasmic stretching with cell adhesion to the substratum. The OMC mediated and promoted cell differentiation from OSC to osteoblast through osteoblastic phenotype cell (OBC) by cell-aggregation of nodules with "pile up" phenomenon of OBC onto OMC. The osteogenesis might be performed by coupling work of both cells, OMC originated from monocyte of HSC and OBC originated from OSC, which were explained by SEM, TEM and fluorescent probe investigation on BFGCs on the test plate of cp titanium plates with different topographies. This osteogenetic process was proved by investigating cell proliferation, DNA contents, cell-adhesion, alkaline phosphatase activity and osteocalcine productivity for cells on the titanium plates with different topographies. The study showed increased osteogenic effects for cells cultured on Ti with increased surface roughness. Possible mechanisms were discussed from a biomechanical perspective.
© *2004 Kluwer Academic Publishers*

1. Introduction

Physical, biochemical and physiological makeup of an individual cell should be determined by both, intrinsic (genetic) and extrinsic (environmental) factors. In the living body, cell differentiation is performed under conditions controlled by various environmental factors of cells, body fluids, fibers, muscle and bone, which are provided as natural scaffolds according to the natural law of ontological development. When biomaterials are implanted into the living tissue, the extrinsic factors of the cellular environment are greatly changed from the natural environment. The shape, function and differentiation of cells neighboring to the biomaterials of synthetic scaffolds are strongly modulated by physico-chemical change of interfacial conditions between cells and biomaterials [1–4]. Cell adhesion to biomaterials (scaffold) can modulate cell-shape and —function and closely relates to cell-growth and cell-differentiation to rebuild new tissue and organ around the biomaterials. The change of cell-shape leads to functional changes in the cell and causes structural reconstruction of cytoskeletal architecture of microtubles and modulates cytokine release, which are shown here by SEM, TEM and fluorescent investigations [5–11]. There have been a lot of *in vitro* studies on cell adhesion, which have used controlled and modulated physico-chemical structure of biomaterials surfaces. In recent years, the topographic dependency of biomaterials upon cell-growth, -orientation, -adhesion and -differentiation have been highlighted. The modulating effect of topography upon cellular responses to biomaterials has been published and has added to knowledge for tissue-engineering [12–18]. In this paper, the mechanism on the accelerating effect of surface roughness upon the osteogenetic activities, such as alkaline phosphatase and bone growth protein will be discussed from the biomechanical standpoint.

*Author to whom all correspondence should be addressed.

2. Materials and methods

2.1. Bone formative group cells

Cell aggregates of bone marrow cells obtained from the femoral bone of beagle were sieved and the sieved aggregates of explants, less than 1 mm^3 were cultured with medium of α-MEM (GIBCO) containing 10% fetal bovine serum (GIBCO), penicillin 100 U/ml and streptomycin 100 μg/ml, in 6-well plastic plate (Dainihonseiyaku, 76-053-05, Osaka, Japan) at 37 °C, 100% humidity and 5% CO_2 95% air. Migrated cells from the explants proliferated and reached confluence at 3 weeks cultivation. The cells were removed from the 6-well plate by rubber scraper and isolated with 0.05% trypsin and Ca, Mg free Hank's solution at room temperature. The isolated cells were seeded in 24-well plastic plate (Dainihonseiyaku, 76-033-05, Osaka, Japan) with the cell density of 50 cells/mm^2. The cells reached confluence at the 7 days cultivation and formed mineralized nodules by the "pile up" phenomenon at 14 days cultivation or more. One well containing bone formative group cells (BFGCs) with high osteogenetic activity was selected from the 24 wells after the 21 days cultivation. The BFGCs were used after 3 passages after 3 weeks in this *in vitro* test.

2.2. Different surface roughness of test plate

A mirror-like smooth surface (Rz 0.6 ± 0.09 μm, Rmax 0.92 ± 0.23 μm) on six cp titanium plates (JIS H 4600, grade 2) was made by barrel polishing (BP) with a TIPTON polishing machine and AT-5, 3P-8 polishing media (Ikeda-seisakusho and Toho-Tech Co., Chigasaki, Japan). Three different surface roughness were prepared by etching the mirror-like surface (BP) for 60 s or 120 s with 4% hydrofluoric acid solution and 15 s pickling of 4% hydrofluoric acid + 8% hydroperoxide solution (4HF 60 or 4HF 120 respectively). The large surface roughness was made by etching BP with 4% hydrofluoric acid solution, 120 s after sand blasting with 0.25–0.5 μm corundum at a pressure of five bars (SB-4HF 120) [4]. Six plates of each BP, 4HF 60, 4HF 120 and SB-4HF 120 were provided for the *in vitro* tests. The surface roughness was measured by mechanical stylus profilometry with Surfcom® (Tokyo Seimitsu, Tokyo, Japan). The topographies were investigated by SEM (Figs. 1 and 2) and measured with 2-D profiles and a scanrange of 1.0–2.0 mm in four directions on each plate (Table I). Titanium film evaporated onto a PMMA plate was used as a control. All test plates were prepared as 10 mm squares with 1.0 mm thickness, and serially rinsed with tap water, distilled water and redistilled water. After that, the test plates were cleaned with sonic vibration for 15 min. in acetone, dried at 60 °C for 3 h and kept in a UV chamber (265 nm) [19].

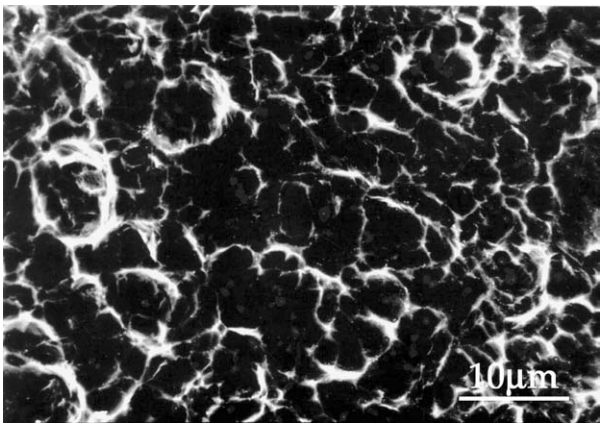

Figure 1 SEM of 4HF 60; Titanium plate etched with 4% hydrofluoric acid solution, 60 s and pickled with 4% hydrofluoric acid +8% hydroperoxide solution, 15 s. Small surface roughness consisted of craters with Ra 0.39 ± 0.01 μm, Rz 2.7 ± 0.18 μm and Sm 2.6 ± 0.3 μm.

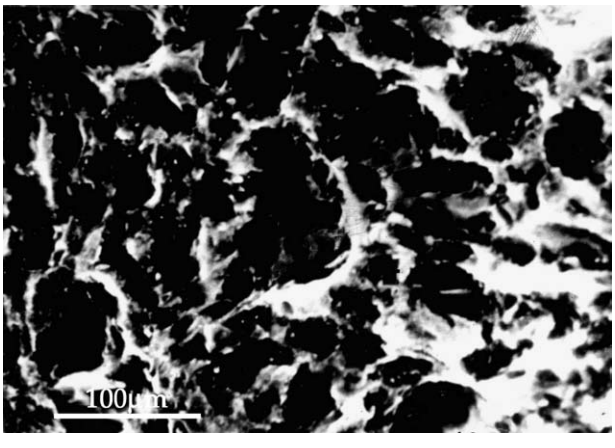

Figure 2 SEM of SB-4HF 120; Titanium plate etched with 4% hydrofluoric acid solution, 120 s and pickled with 4% hydrofluoric acid +8% hydroperoxide solution, 15 s after sand blasting, large surface roughness, Ra 1.8 ± 0.12 μm, Rz 10.58 ± 0.53 μm and Sm 36 ± 9.0 μm.

TABLE I Titanium plate etched with hydrofluoric acid

Treating method	Ra (μm)	Rz (μm)	Rmax (μm)	Sm (μm)
Barrel polishing		0.6 ± 0.09	0.92 ± 0.23	Blow-vestiges and scratches
4HF 60 sec.	0.39 ± 0.01	2.7 ± 0.18	3.3 ± 0.38	2.6 ± 0.3
4HF-8H_2O_2 15 sec.				
4HF 120 sec.	0.57 ± 0.02	3.5 ± 0.21	5.1 ± 0.50	4.8 ± 0.5
4HF-8H_2O_2 15 sec.				
Corundum blasting at 5 bars	1.87 ± 0.12	10.58 ± 0.53	25.1 ± 8.01	36 ± 9.0
4HF 120 sec.				
4HF-8H_2O_2 15 sec.				
Ti plasma spray coating	4.86 ± 0.41	31.28 ± 3.4	46.6 ± 8.7	48 ± 11

4HF: 4% hydrofluoric acid solution, 4HF-8H_2O_2: 4% hydrofluoric acid +8% H_2O_2 solution, sec.: etching time, Corundum: average grain size, 0.38 ± 0.18 μm, Ra: center line average height, Rz: average value of the heights at the five highest peaks and the depths of the five deepest valleys, Rmax: maximum peak-valley hight, Sm: average of space between the peak-flanks on the mean line, Number: average $\pm$ sample standard deviation, $n = 6$ titanium plates (10×10 mm).

2.3. Morphological investigation of BFGCs

BFGCs on the test plates were viewed by fluoresceindiacetate staining and SEM. The microstructures, release of lysosomal enzymes and cytoskeleton (actin and tubulin) were observed by TEM and immunofluorescence imaging [20].

2.4. Osteogenetic activity of BFGCs

Osteogenetic activity of BFGCs on the test plates with different surface roughness was investigated by four parameters of cell-number, DNA content, alkaline phosphatase activity (ALP) and bone growth protein (BGP).

2.4.1. Counting method of living BFGCs on the test plate

The living cells were distinguished from the dead cells by fluoresceindiacetate staining and fluorescence microscopy at 470–490 nm (Nikon, Tokyo, Japan) [19, 21] and the cell numbers on the test plate were counted using a photo-pattern analyzer, CELCOM (Aoi-system, Osaka , Japan) [22].

2.4.2. Assay of DNA content, ALP activity and BGP production

The adhered cells on the test plate were rinsed three times with 5mM HEPES (N-2-hydroethyl pierazine-N-ethane sulfonic acid) buffer solution (pH 7.4). The adhered cells were detached from the test plate and homogenized in the HEPES solution by supersonic vibration at 1961 KHz, 10 V, 2 min (ICM, Osaka, Japan). The homogenized solution was used as the test sample for each essay of DNA, ALP and BGP.

DNA content: According to the Hinegardner method [23], 3,5-diaminobenzoic acid dihydrochloride (Aldrich Chem. Co., Milwaukee, US) was added to the test sample and reacted at 60 °C, 45 min. The reaction was stopped with 1N HCl. The DNA contents in each test sample were measured at 600 nm with a spectrophotometer and read by comparing with DNA standard of calf-thymus (Sigma Chem. Co., St. Luis, US).

ALP activity: Sigma kit for ALP assay using pNPP (p-nitrophenyl phosphate) (Sigma Chem. Co. St. Luis, US) was utilized according to the methods described by Bessey and Lowry [24, 25]. The enzymic reaction between the test samples and pNPP was performed at 37 °C, 30–60 min and stopped with 3 N NaOH. The ALP activity of the test sample was determined by spectrophotometry, at 410 nm and compared with that of a pNPP standard.

BGP production: After the 2 h pre-reaction of the test sample with a Gla-OC antibody coated microtiter plate (Takara Medicals, Shiga, Japan), the antibody labeled with a peroxidase conjugate was reacted with Gla-OC at 20–30 °C, 3 h. The reacted test samples were treated with a substrate of tetramethylbenzene solution at 20–30 °C, 15 min. The BGP productions were measured at 410 nm in a spectrophotometer and read by comparing to that of the standard, bovine osteocalcine [26].

2.5. Adhesive strength

Supersonic vibration is a simple and effective method to measure cell adhesive strength because of just mechanical detachment by supersonic disturbance to sandwich layer at the cell/substratum interface [4, 27–30]. Cell adhesive strength of BFGCs to substratum with different surface roughness was measured by supersonic vibration of 485 KHz, 5 V and 30 s at 2, 4, 7, 14 and 21 days cultivation [27].

3. Results

Bone formative group cells (BFGCs) consist of a mixed population of osteogenetic stem cells (OSC) and hematopoietic stem cell (HSC). Many cells at each biogenetic stage of OSC and HSC differentiation cascade are present, thus bone formation should be observed on the test plates, because BFGCs were collected from the nodules of cell-aggregations consisting of HSC and OSC with various stages of their differentiating cascade.

3.1. Bone formation on evaporated titanium film

The cellular response of BFGCs to the evaporated titanium film (Ti-film) demonstrated closer cell-adhesions with more cytoplasmic stretching with the lapse of culture time. At 24 h cultivation the cells bestowed biomechanical stimuli of tensile stress in their cytoplasm with cytoplasmic stretching (Figs. 3–5). When the proliferation of BFGCs reached confluence at 10 days cultivation they demonstrated the “pile up” phenomenon and nodule formation (Figs. 6 and 7). Cross section of the nodule demonstrated the piled up BFGCs, consisting osteomediator cell (OMC) and osteoblastic cells (OBC). These cells are named expediently according to their position on the Ti-film, e.g., direct contact to substratum (OMC) or piled up cell to cell contact (OBC) (Figs. 8 and 9). Close adhesion of BFGCs to the Ti-film gave rise to parallel alignment of ER, MT and flow of electro-dense nano-particles to the substratum of Ti-film (Figs. 5 and 10). The adhered cell is supported by the intracellular filamentous network of cytoskeletons, including microtubles, intermediate filaments and actin filament (Figs. 11–13).

3.2. Osteomediator cell from HSC

Phagocytic monocytes in the HSC population differentiated to macrophages when the medium used for L929 was added to the culturing medium for BFGCs after 7 days. The microtubules and lysosomal enzymes were distinctly detected by immunofluorescence imaging compared to that without any addition of the L929 used medium (Figs. 12 and 13). Monocyte adhered to the substratum under the specialized circumstance such as overpopulation and high cell density of the “pile up” phenomenon may load to the development of cell-differentiation from monocyte of the HSC to OMC.

Figure 3 Bone formative group cells (BFGCs) contacted and adhered to evaporated titanium film (Ti-film), 24 h cultivation.

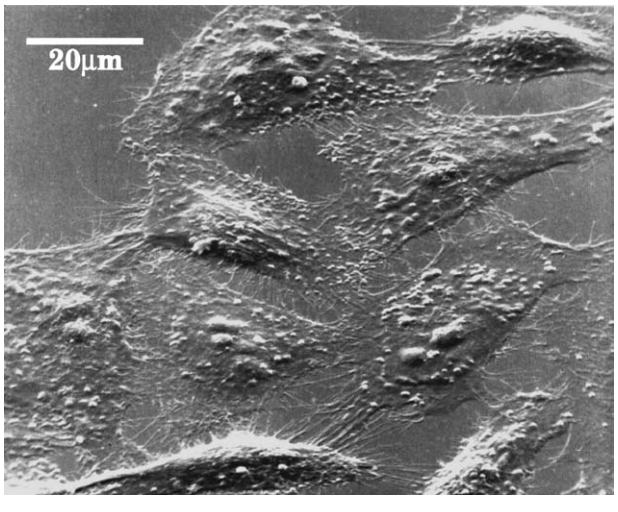

Figure 4 SEM demonstrates BFGCs adhered closely to evaporated Ti-film with their cytoplasmic spreading, 24 h cultivation.

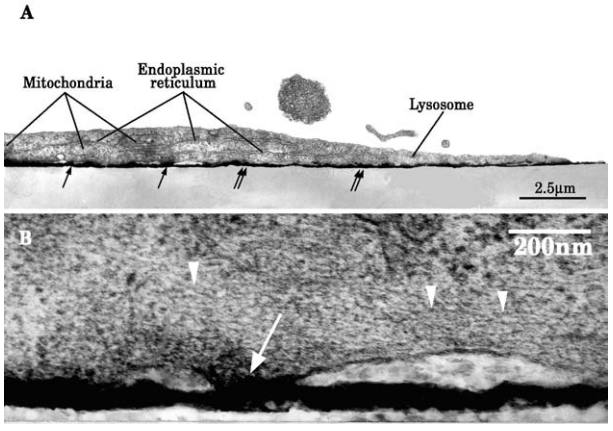

Figure 5 (A) TEM of BFGCs demonstrates the spreading adhesion to the Ti-film with the cell to metal fusion (↑↑) and focal contact (↑). Endoplasmic reticulum, mitochondria and other cell organella run parallel with the substratum. (B) Large magnification demonstrates parallel net work of electro-dense filaments (▽) to the substratum of Ti-film and dispersions of electro-dense particles from the focal contact into the cytoplasm (↓).

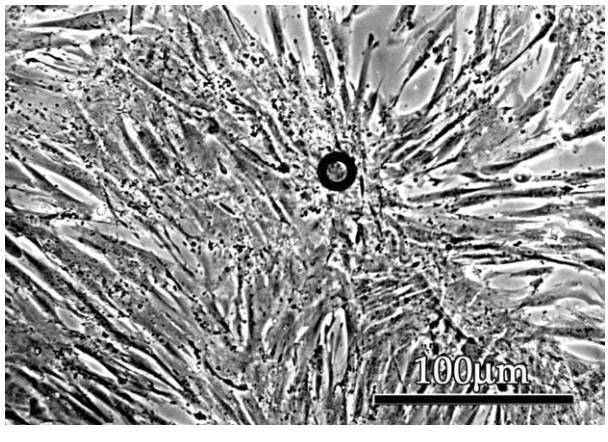

Figure 6 Early stage of nodule formation (○) on Ti-film, BFGCs demonstrate nodule formation of "pile up" phenomenon with cell aggregate, 10 days cultivation.

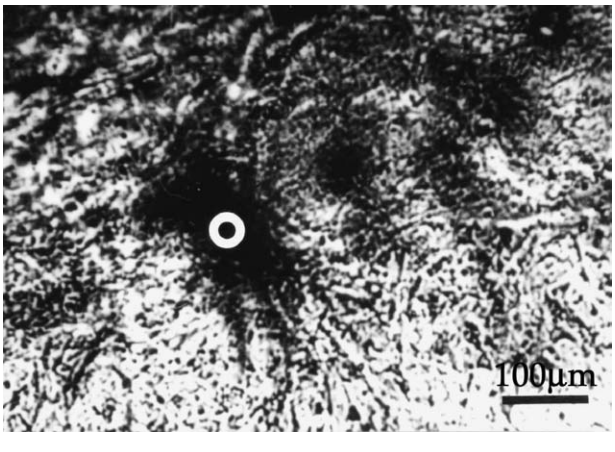

Figure 7 Nodule formation (○) with cell aggregate of piled up BFGCs, 14 days cultivation on Ti-film.

3.3. Bone formation and surface roughness

3.3.1. Cell growth rate and DNA

Morphological responses of BFGCs to the test plates with different surface roughness were investigated by SEM. The cells adhered closely to the mirror-like surface of BP (Fig. 14), and the cell orientation was not changed with scratched grooves of a depth 0.6–1.9 μm and width 0.3–2.5 μm (Fig. 15) as well as small surface roughness of Ra 0.39 μm Rz 2.7 μm Rmax 3.3 μm Sm 2.6 μm of 4HF 60 (Fig. 16).

Fluoresceindiacetate staining demonstrated the polygonal cell shape closely adhered to the BP test plates (Fig. 17). On the contrary, the cells demonstrated a comparatively round shape and early nodule formation at the bottom of craters on samples with large surface roughness, Ra 1.87 μm Rz 10.58 μm Rmax

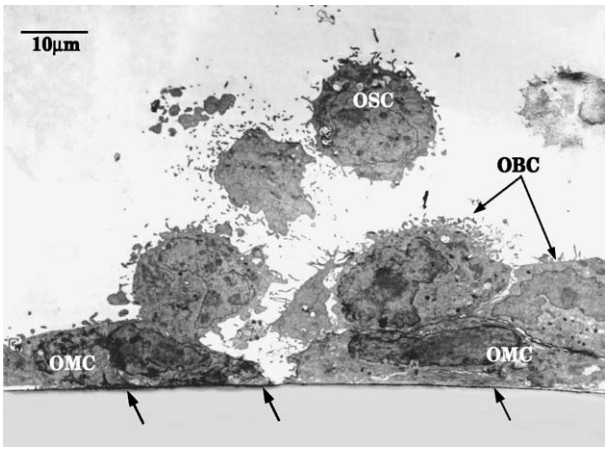

Figure 8 Cross section of the nodule demonstrates the piled up BFGCs on Ti-film. The adhered monocytes differentiate to osteo-mediator cell (OMC), and osteoblastic phenotype cell (OBC) closely contacted to the OMC, 10 days cultivation on Ti-film (arrow).

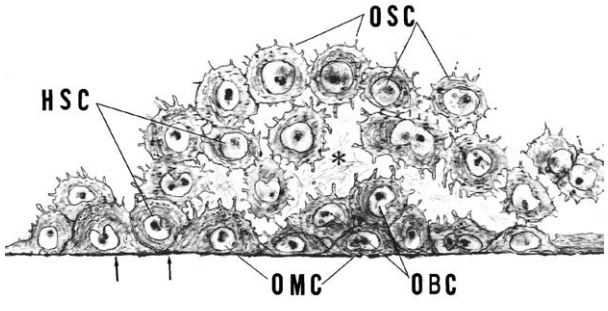

Figure 9 Schema of the nodule consisted of OSC, OBC, OMC, HSC, extracellular matrix and collagen fiber (∗) on Ti-film (arrow).

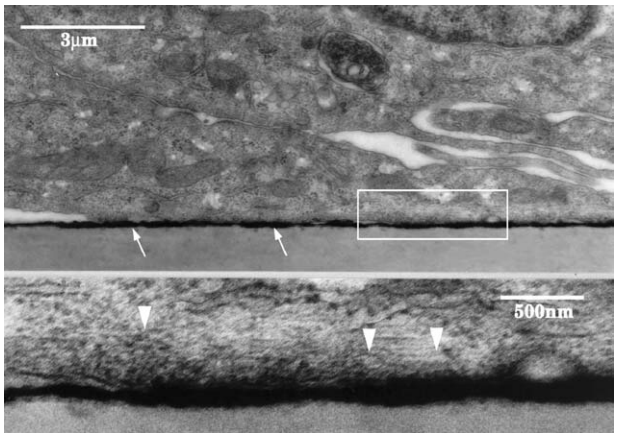

Figure 10 Upper: Cross section of Fig. 6, close adhesion of OMC to Ti-film (arrow) and piled up OBC. Lower: Large magnification of upper photo, parallel alignment of ER, MT and cell-organella caused by cytoplasmic stretching of the cell adhesion. Electrodense nano-particles (10–20 nm) constructing cytoskeleton demonstrate parallel flow to the substratum (aoorw head), referring to Fig. 5.

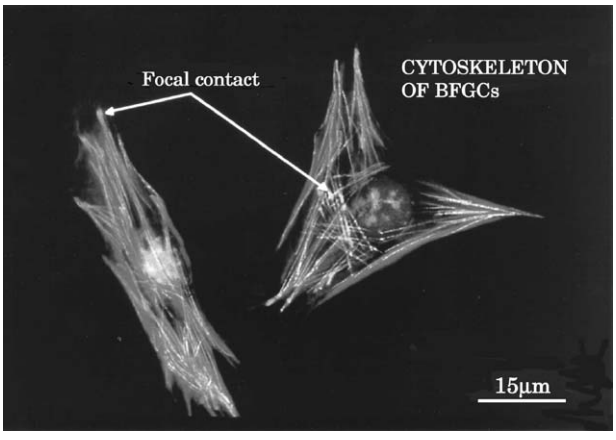

Figure 11 Cytoskeleton of BFGCs adhered closely to the substratum, fluorescent probing with rhodamine phalliodin for F-actin filaments and DAPI (46-diamino-2-phenylindol dihydrochloride) for nucleus, focal contact (minor modification by computer graphics).

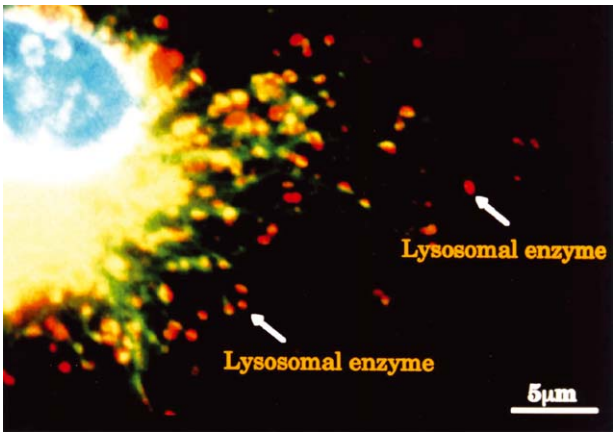

Figure 12 Macrophage differentiated from monocyte of BFGCs by adding the 7 days cultured medium of L929 cells into the culture medium for BFGCs demonstrates active production of microtubules and lysosomal enzymes, detected by immunofluorescence imaging.

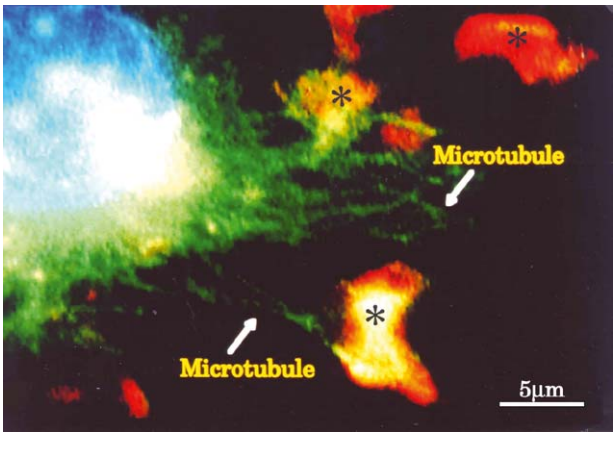

Figure 13 Microtubules and F-actin of microvilli (∗) are distinct but not clear in the lysosomal enzymic release in the monocyte without the addition of L929 cultured medium.

25.1 μm Sm 36 μm of SB-4HF 120 at 7 days of cultivation (Figs. 18 and 19), and the cell proliferation was significantly checked on the large surface roughness, as follows.

The cell growth rate and DNA contents increased with culture day, and reached the highest level at 10 days cultivation. Higher levels of cell density and DNA content were seen on the Ti-film, mirror-like surface and small surface roughness (4HF 60) compared with that of large surface roughness of 4HF 120 and SB-4HF 120 (Fig. 20). Significant differences between the both DNA contents of rough surface (4HF 120 and

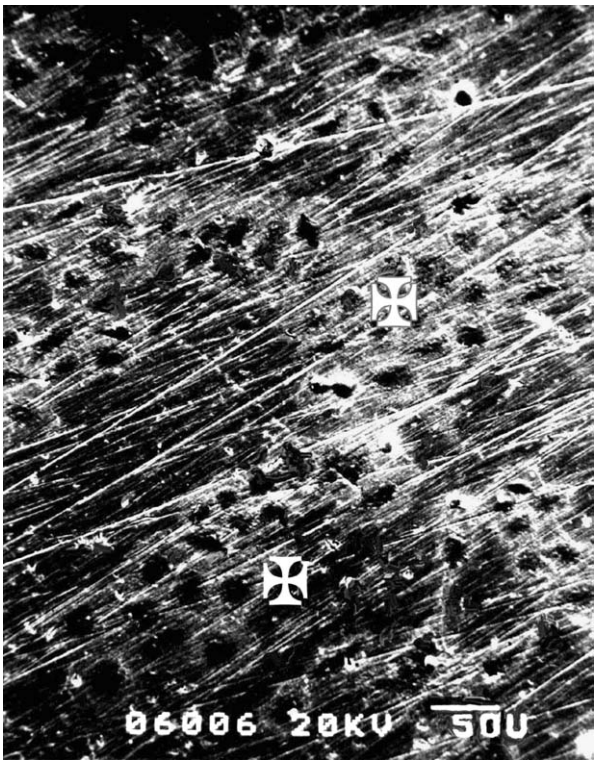

Figure 14 SEM of BFGCs adhered closely to the barrel polished mirror-like surface of titanium, 72 h cultivation. Cell growth and colony (✠) developed normally without any interference of polishing scratches.

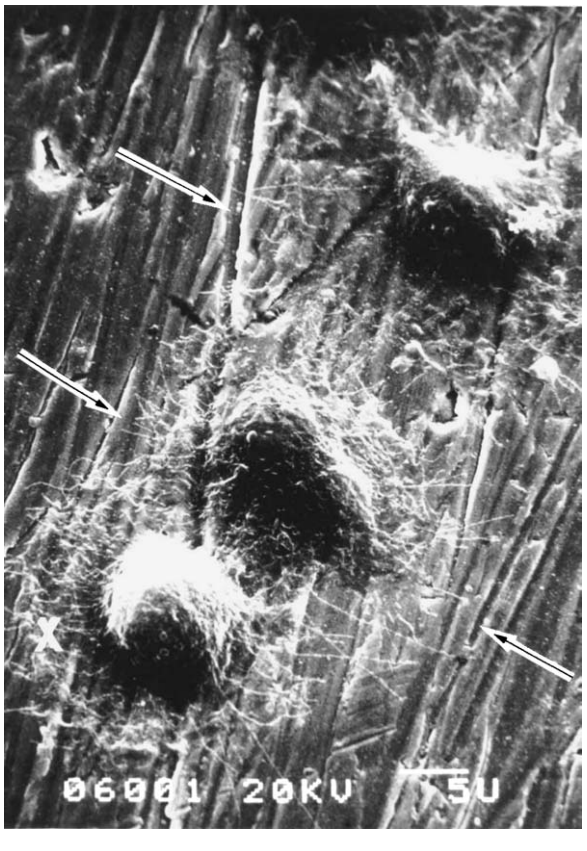

Figure 15 Large magnification of BFGC on barrel polished surface, cell adhesion without any interference of scratched microgrooves, depth 0.6–1.9 μm, width 0.3–2.5 μm (arrow), 72 h cultivation.

SB-4HF 120) and smooth surfaces (Ti-film and BP) were distinct after 7 and 18 days cultivation, while no significant difference was assessed at the 21 days cultivation (Fig. 21).

Figure 16 SEM of BFGC adhered to Ti plate with small roughness (4HF 60), the small craters demonstrate no interference to the cytoplasmic extruding of pseudopodia and filopodia.

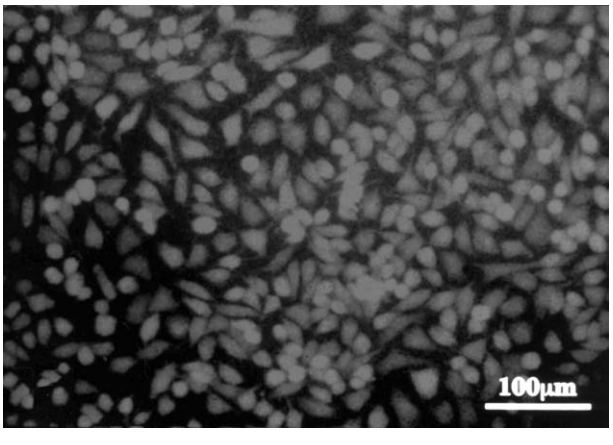

Figure 17 Normal shape of BFGCs adhered to the barrel polished surface, 7 days cultivation, fluoresceindiacetate staining.

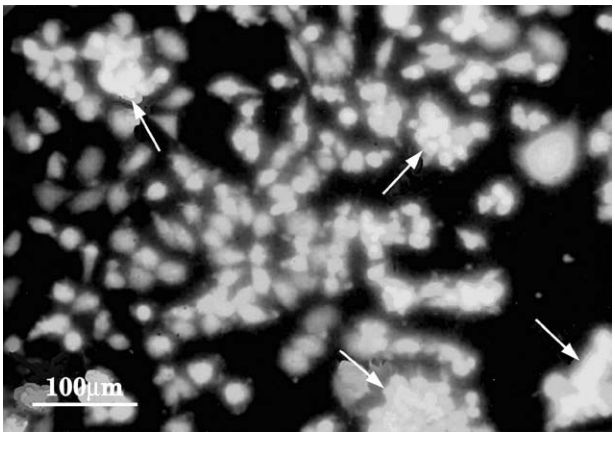

Figure 18 Relatively round shape of BFGCs on the large surface roughness of SB-4HF 120, early stage of "pile up" phenomenon at the bottom of crater (arrow), 7 days cultivation, fluoresceindiacetate staining.

Figure 19 SEM of pilled up FBGCs at the bottom of large crater of the large surface roughness, SB-4HF 120.

3.3.2. ALP activity and BGP production

BGP on the mirror-like surface and 4HF 60 demonstrated almost the same levels to those of the control, Ti-film. On the contrary, the large roughness of the SB-4HF 120 demonstrated that the ALP and BGP reached the highest peak at the early stage of 10 days cultivation (Figs. 22 and 23).

In short, BFGCs on SB-4HF 120 performed the "pile up" phenomenon at the early stage of 7 to 10 days cultivation whilst the growth rate was slowed. ALP activity and BGP production were significantly accelerated. However, ALP and BGP production on the other samples caught up by 21 days of culture.

3.4. Cell adhesive strength to different topographies

Adhesive strength of BFGCs to the test plates with various sizes of surface roughness was measured by supersonic vibration of 485 KHz, 5 V, 30 s. Generally, large surface roughness demonstrated a lower adhesive strength to BFGCs. However, no significant difference was recognized in the statistical investigations between each surface roughness of BP, 4HF 60, 4HF 120 and SB-4HF 120, except between BP and SB-4HF 120 at 21 days cultivation (Fig. 24).

4. Discussion

4.1. Osteogenesis

In vivo examinations have clarified that osteogenesis originates from both sides of implant's surface and host-bone's surface, constructing the implant-sheath-bone surrounding the implant. Scientific evidence of osteomediator cell (OMC) presence has been proved by TEM investigation on animal experiments [4, 31, 32]. This *in vitro* study could trace the process of osteogenesis around the titanium implant and the cell differentiation from bone formative group cells (BFGCs) to OMC and OBC *in vivo*. The driving force for the cell-differentiation caused by a biomechanical stress of cytoplasmic tension of cell adhesion to the substratum and the "pile up" phenomenon of cell to cell adhesion were conjectured [31, 33]. The nodules of BFGCs consisted of OBC originated from OSC and OMC differentiated from phagocytic monocytes originated from HSC (Figs. 8 and 9).

Larsson *et al.* reported that implant-adherent macrophages are detected prior to bone formation at the surfaces of materials inserted in bone [34]. The macrophages are long-lived, versatile cells and have a pivotal role at the surfaces of implanted materials with

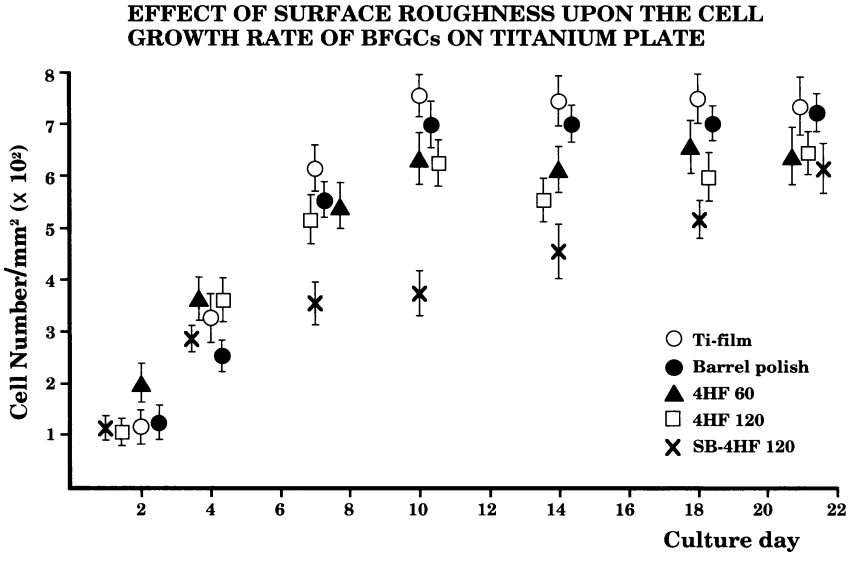

Figure 20 Cell growth rate of BFGCs on titanium plate with different surface roughness: ○ Ti-film, ● Barrel polish, ▲ 4HF 60, □ 4HF 120, ✕ SB-4HF 120. The error bar represents sample standard deviation, $n = 6$.

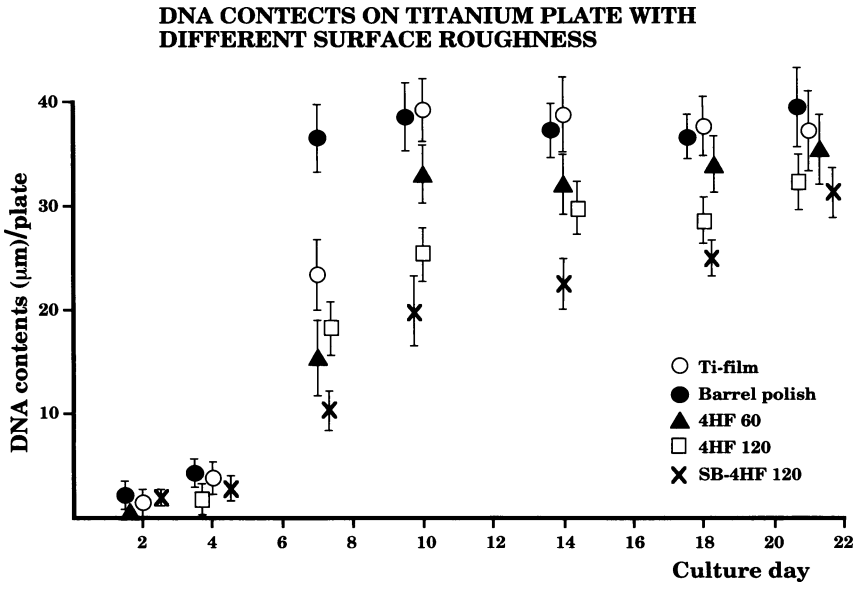

Figure 21 DNA contents on titanium plate with different surface roughness: ○ Ti-film, ● Barrel polish, ▲ 4HF 60, □ 4HF 120, ✕ SB-4HF 120.

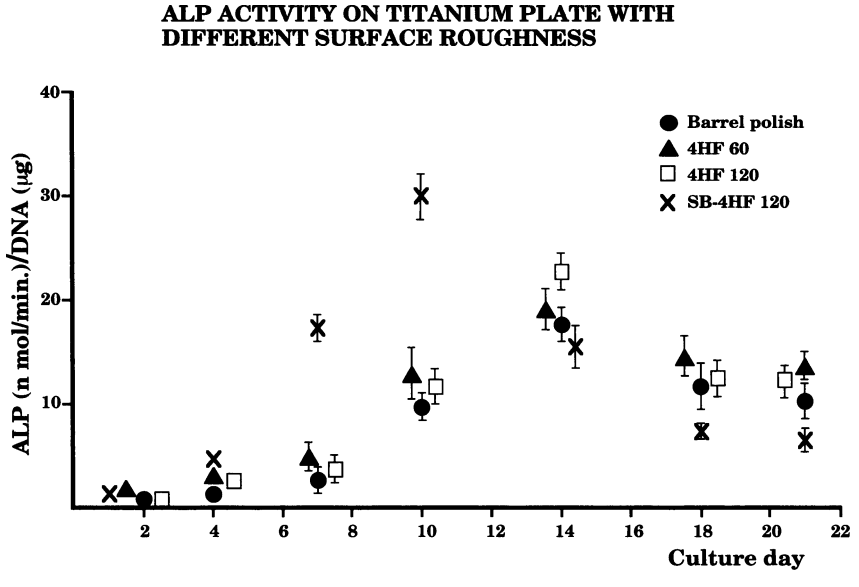

Figure 22 ALP activity on titanium plate with different surface roughness: ● Barrel polish, ▲ 4HF 60, □ 4HF 120, ✕ SB-4HF 120.

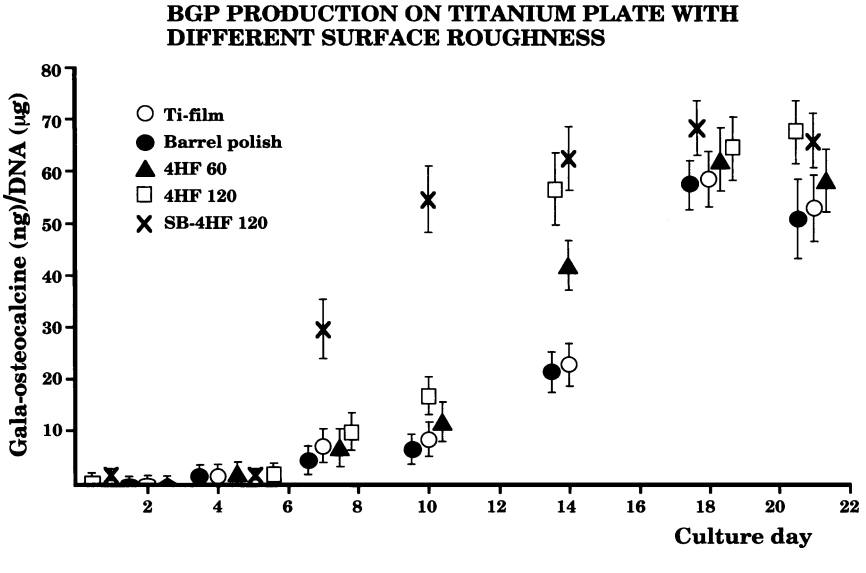

Figure 23 BGP production (bone growth protein, Gla-osteocalcine) on titanium plate with different surface roughness: ○ Ti-film, ● Barrel polish, ▲ 4HF 60, □ 4HF 120, ✕ SB-4HF 120.

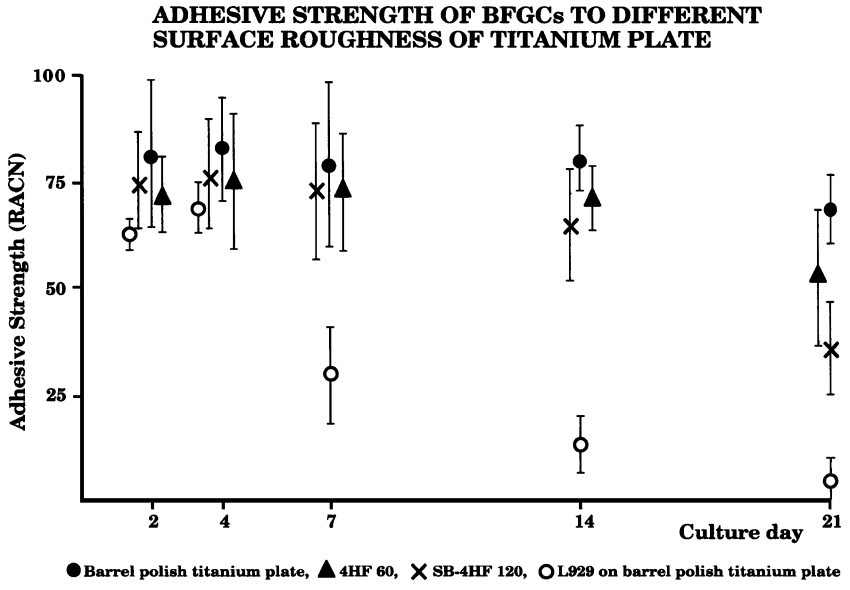

Figure 24 Adhesive strength of BFGCs and L929 to titanium plate with different surface roughness: ● Barrel polish, ▲ 4HF 60, ■ SB-4HF 120, ○ L929 on barrel polish, RACN (relative adhered cell number), RACN $= \frac{\text{Number of adhered cells after sonic vibration}}{\text{Number of adhered cells before sonic vibration}}(\%)$

the participation of down-regulators or up-regulators for tissue demolition, for example IL-10, IL-4, IFN-r and growth factors (down) or IL-6, IL-11, TNF-α and PGE_2 (up), which are controlled with surface chemistry and topography of biomaterials [35]. This *in vitro* data suggested that monocyte of HSC differentiated to macrophages (or osteoclasts) with a bone destructive factor or to OMC with a bone growth factor, according to the environmental conditions of the cell. Phagocytic monocyte of HSC in bone marrow has pulripotentiality and allows a balance of bone formation or resorption. It is revealed that the phagocytic monocyte adhered directly to the substratum differentiated to OMC as metamorphosis on the way through a differentiating cascade from monocyte to macrophage and release growth factor of cytokine for the differentiation from OSC to OBC and finally osteoblast. Therefore the osteogenesis around the implant should be performed by a group function of BFGCs, consisted of OBC from OSC and OMC from HSC. When the monocytes adhere to the substratum, the cells are differentiated to OMC by mechanical stimulation with cytoplasmic tension caused by cell-adhesions. Close contact and adhesion of OSC onto the OMC with "pile up" phenomenon promote the cell differentiation from OSC to OBC, finally to osteoblast by releasing growth factors and cytokine from the OMC [32]. Cytokine release from OMC to OBC may be encouraged by biomechanical stimulation with cytoplasmic tension from cell adhesion to the substratum. Such bone forming process has been discussed from a biomechanical standpoint *in vitro* and *in vivo* examinations, which reported that mechanosensitivity of bone was controlled with mechanostate gene-expression on/off, in osteogenic stem cells. The cells may differentiate to osteoblasts with the tensile strain of 100–1000 $\mu\varepsilon$. Mechanical stress converts to chemical energy for gene expression of cell differentiation from OSC to osteoblast with cytoplasmic tension or osteoclast with cytoplasmic compression [33, 36].

4.2. Bone formation and topography

Many *in vitro* studies on the effect of surface topography upon cell-adhesion, -proliferation and -differentiation have been reported [12–18, 37–42]. Martin *et al.* suggested that implant surface roughness may play a role in determining phenotypic expression of cells from the *in vivo* and *in vitro* data [14]. Anselme *et al.* proposed an attempt at modelization of the cell-surface interaction including the influence of a fractal dimensions parameter and reported that cultured human osteoblasts prefered surfaces with relatively high micro-roughness amplitude and with a low level of repeatability [15, 16]. Perizzolo *et al.* indicated that surface topography and chemistry could affect osteogenesis and interactions between chemistry and topography could occur [17]. Boyan *et al.* reported that both Cox-1 and Cox-2 were involved in the response of osteoblasts to surface roughness with respect to production of PGE_2 (prostaglandin dinoprostone), TGF-β1 (tissue growth factor) and osteocalcine [18].

4.3. What's the reason for the acceleration of osteogenesis on the rough surface?

Anselme *et al.* reported used large fractal dimensions and developed surfaces that controlled the cell proliferation and adhesion of human osteoblast but accelerated the ALP and BGP activities [15]. So far, however, there is no explanation on the accelerating mechanism of osteogenesis caused by large surface roughness of large fractal dimensions. *In vitro* studies suggested that the cells demonstrated a slow speed of growth rate and could not cross over large grooves, glens, holes, and craters of large surface roughness, while the acceleration of ALP activity and BGP production was achieved by reaching confluence faster and entering into the "pile up" phenomenon resulting in nodule formation at the bottom of holes, craters, glens and slits, because the bottom is a limited narrow space.

4.4. Adhesive strength to substratum

Comparative evaluation on five different measuring methods on cell adhesive strength has been reported in the literature [27]. (1) Method of plating efficiency after trypsinization is a simple and generalized parameter but not accurate, because it is not natural state, due to deterioration of sandwich layer at the cell-substratum interface by trypsinization. (2) Measurement of cell contact angle to substratum can indicate the cell wettability but it is not adhesive strength [43]. Greatest shortcoming is complicated procedure for measurement, although this is effective method to conjecture cytoplasmic tension of adhered cell. (3) Measurement by centrifugal force to adhered cell is a doubtful method, because the cell nucleus breaks out of the unit membrane leaving residual fragments of cytoplasm and unit-membrane on the substratum [27]. (4) Viscometric method using shear stress of medium-flow to adhered cells, can measure real value of cell adhesive strength but it is not convenient for large samples, due to the complicated procedure [44–47]. (5) Method of supersonic vibration is simple and useful to measure cell adhesive strength numerically, due to the detachment caused by mechanical disturbance to the sandwich layer at cell/substratum interface [27–29]. Adhesive strength of cell to metallic substratum depends upon the microarchitecture of sandwich layer at the cell/substratum interface, consisting of proteoglycans cohesion of extracellular matrix, including focal contact, podosome, hemidesmosome and cell to metal fusion [48]. These biopolymers were effectively disturbed by the vibration of 485 KHz, may be tuned to proper vibration of the biopolymers.

According to the previous reports, supersonic vibration was utilized in this study. Adhered cells are more detachable from substratum with the length of culture. Cell density, 50 cells/mm^2 inoculated cells, demonstrated the highest adhesive strength at 2 to 4 days of cultivation, after that the adhesive strength decreased gradually with the culture day. When the cells reached the confluence at 2000 cells/mm^2 or more, the cells detached from the substratum themselves, because of insufficient supply of growth nutriments and gasses. It is revealed that the cells detach themselves from substratum under the sublethal condition of overpopulation, which causes deterioration of the sandwich layer at the cell-substratum interface by releasing lysosomal enzymes to escape from the crisis of overpopulation. Larger surface roughness demonstrates lower adhesive strength of cells, smaller proliferation, and higher ALP activity and BGP production, because the rougher surface reaches to higher cell-density and performs the "pile up" phenomenon at an earlier stage of cell-cultivation, in the narrow space at the bottom of craters, holes and valleys, compared with those of smooth surface. However, these accelerating effects of the large surface roughness upon ALP and BGP dissolve at the final stage of 21 days cultivation. It suggests that special attention should be paid to long term investigation of clinical trial tests.

5. Conclusion

In vitro study using bone formative group cells (BFGCs) of wild type strain derived from bone marrow of beagle's femur demonstrates that osteogenesis is performed on the titanium plate by the joint work of BFGCs with the "pile up" phenomenon, consisted of osteomediator cell (OMC) differentiated from phagocytic monocyte of hematopoietic stem cells (HSC) and osteoblastic phenotype cell (OBC) originated from osteogenic stem cells (OSC). Phagocytic monocytes may differentiate to OMC by mechanical stress of cytoplasmic tension with direct cell adhesion to the titanium plate. The OMC may mediate and promote cell differentiation from OSC to osteoblast through OBC.

At least two performances are required for the purpose of promoting the osteogenesis *in vitro*, one is close cell adhesion with cytoplasmic stretch to the substratum, and the other is "pile up" phenomenon of wild type strain cells, BFGCs. The osteogenetic process is accelerated with larger surface roughness, due to early development of "pile up" phenomenon, in spite of lower level in cell growth rate and cell-adhesiveness.

Acknowledgments

Financial support for this study was provided by a grant from the Training Institute of the Japanese Society of Oral Implantology. The authors would like to thank Ms. Yoshiko Ohta, Mr. Jo Inoue and Dr. Yoshihisa Tamai for their helpful suggestions and assistance in this study.

References

1. H. KAWAHARA, M. KOBAYASHI, S. MORIWAKI, Y. TAKASHIMA and T. IWAO, *J. Oromax. Biomech.* **1** (1995) 11.
2. R. B. O'NEAL, J. J. SAUK and M. J. SOMERMAN, *J. Oral Implantol.* **18** (1992) 243.
3. M. HORMIA and M. KONOMEN, *J. Periodontal Res.* **29** (1994) 146.
4. H. KAWAHARA, in "Encyclopedic Handbook of Biomaterials and Bioengineering," Part B, edited by D. L. Wise, D. J. Trantolo, D. E. Altobelli, M. J. Yaszemski, J. D. Gresser and E. R. Schwartz (Marcel Dekker Inc., New York, 1995) Vol. 2, p. 1469.
5. R. ZHANG, S. C. SUPOWIC and G. L. KLEIN, *J. Bone Miner. Res.* **10** (1995) 415.
6. K. BURRIDGE and M. CHRZANOWSKA-WODNICKA, *Ann. Rev. Cell Dev. Biol.* **12** (1996) 463.
7. G. GRONOWITES and M. B. MCCARTHY, *J. Orthop. Res.* **14** (1996) 878.
8. R. K. SHINHA and R. S. TUAN, *Bone.* **18** (1996) 451.
9. L. NISSINEN, L. PIRILA and J. HEINO, *Exp. Cell Res.* **230** (1997) 377.
10. M. M. KLINGER, F. RAHEMTULLA, C. W. PRINCE, L. C. LUCAS and J. E. LEMONS, *Crit. Rev. Oral Biol. Med.* **9** (1998) 449.
11. A. LETIC-GAVRILOVIC, R. SCANDURRA and K. ABE, *Dent. Mater. J.* **19** (2000) 99.
12. R. SINGHVI, G. STEPHANOPOULOS and D. I. C. WANG, *Biotechnol. Bioeng.* **43** (1994) 764.
13. H. LIAO, A.-S. ANDERSSON, D. SUTHERLAND, S. PETRONIS, B. KASEMO and P. THOMSEN, *Biomater.* **24** (2003) 649.

14. J. Y. MARTIN, Z. SCHWARTS, T. W. HUMMER, D. M. SEHRAUB, J. SIMPSON, J. LANKFORD JR., D. D. DEAN, D. L. COCHRAN and B. D. BOYAN, *JBMR* **29** (1995) 389.
15. K. ANSELME, M. BIGERELLE, B. NOËL, E. DUFRESNE, D. JUDAS, A. IOST and P. HARDOUIN, *ibid.* **49** (2000) 155.
16. K. ANSELME, M. BIGERELLE, B. NOËL, A. IOST and P. HARDOUIN, *ibid.* **60** (2002) 529.
17. D. PERIZZOLO, W. R. LACEFIELD and D. M. BRUNETTE, *ibid.* **56** (2001) 498.
18. B. D. BOYAN, C. H. LOHMANN, M. SISK, Y. LIU, V. L. SYLVIA, D. L. COCHRAN and D. D. DEAN, *ibid.* **55** (2001) 350.
19. D. KAWAHARA, Y. KIMURA, M. NAKAMURA and H. KAWAHARA, *Clin. Mater.* **14** (1993) 229.
20. N. ARAKI, T. HATAE, T. YAMADA and S. HIROHASHI, *J. Cell Sci.* **113** (2000) 3329.
21. G. SCHMALZ and L. NETUSCHIL, *JBMR* **19** (1985) 653.
22. H. KAWAHARA, K. IMAI and D. KAWAHARA, *Int. Endodont. J.* **21** (1988) 100.
23. R. T. HINEGARDNER, *Anal. Biochem.* **39** (1971) 197.
24. O. A. BESSY, O. H. LOWRY and M. J. BROOK, *J. Biol. Chem.* **164** (1946) 321.
25. O. H. LOWRY, N. R. ROBERTS, M. L. WU, W. S. HIXON and E. J. CRAWFORD, *ibid.* **207** (1954) 19.
26. Y. FUKUTA, *J. JOMS* **44** (1998) 42.
27. Y. MIMURA, K. HASHIMOTO and H. KAWAHARA, *J. Oromax. Biomech.* **4** (1998) 48.
28. T. MAEDA, H. TAGUCHI and H. KAWAHARA, *J. JDMD* **22** (1981) 162.
29. K. IMAI, M. NAKUMURA and H. KAWAHARA, Transaction of the Tissue Culture Society for Dental Research, No. 16, 1979, 9.
30. H. KAWAHARA, in "Oral Implantology," edited by H. Kawahara (Ishiyaku Pub. Inc., Tokyo, 1991) p. 171.
31. H. KAWAHARA, T. NAKAMURA, Y. TAKASHIMA, K. HASHIMOTO and H. TAKEUCHI, *J. Oromax. Biomech.* **1** (1995) 17.
32. H. KAWAHARA, *JJSB* **18** (2000) 3.
33. H. ZREIQAT, P. EVANS and C. HOWLETT, *JBMR.* **4** (1999) 389.
34. C. LARRSON, M. ESPOSITO, H. LIAO and P. THOMSEN, in "Titanium in Medicine," edited by D. M. Brunette, P. Tengvall, M. Textor and P. Thomsen (Springer, Berlin, 2001) p. 587.
35. P. THOMSEN and C. GRETZER, *Curr. Opin. Solid State Mater. Sci.* **5** (2001) 163.
36. H. KAWAHARA, D. KAWAHARA, M. HAYAKAWA, Y. TAMAI, T. KUREMOTO and S. MATSUDA, *Implant Dent.* **12** (2003) 61.
37. R. BIZIOS, *Biotechnol. Bioeng.* **43** (1994) 582.
38. K. C. DEE and R. BIZIOS, *ibid.* **50** (1996) 438.
39. L. F. COOPER, T. MASUDA, P. K. YLIHEIKKILA and D. A. FELTON, *Int. J. Oral. Maxillofac. Implants.* **13** (1998) 163.
40. J. E. DAVIES, *Anat. Rec.* **245** (1996) 426.
41. K. WEBB, V. HLADY and P. A. TRESCO, *JBMR* **49** (2000) 362.
42. Z. SCHWARTS and B. D. BOYAN, *J. Cell Biochem.* **56** (1994) 340.
43. H. KAWAHARA, *Int. Dent. J.* **18** (1968) 443.
44. H. KAWAHARA, T. MAEDA, T. ISEKI and A. SÁNCHEZ, *JJSB* **2** (1984) 53.
45. H. KAWAHARA, in "Design of Multiphase Biomedical Materials," edited by K. Tsuruta (Special project supported by the Ministry of Education, Tokyo, 1985) p. 239.
46. H. KAWAHARA, Y. MIMURA and Y. SOEDA, in "Oral Implantology and Biomaterials," edited by H. Kawahara (Elsevier, Amsterdam, 1989) p. 159.
47. H. KAWAHARA and T. MAEDA, *JJSB* **2** (1984) 177.
48. H. KAWAHARA, *Int. Dent. J.* **33** (1983) 350.

Received 19 August 2003
and accepted 20 May 2004